Ionospheric Calibration with SPAM

Huib Intema
Leiden Observatory

SPAM overview

- Source Peeling & Atmospheric Modeling
- Ionospheric calibration & imaging software
- Determines direction-dependent phase corrections
- Applies corrections while imaging & deconvolving
- Applicable to both compact and extended arrays
- Applicable to varying ionospheric conditions

Can SPAM approach work for MS^3?

- In principle YES
  - SPAM calibration has improved the image quality of 74 MHz VLA-A data (35 km, 1.5 MHz BW) and 150 MHz GMRT data (30 km, 6 MHz BW) as compared to self-cal. and field-based cal.
- But...
  - No absolute calibration accuracy available
  - DR in applications limited to $\sim 10^3$
  - Many simplifying assumptions
  - Off-line processing
  - LOFAR calibration problem is more complex (e.g. multiple variable complex beams, large BWs)

SPAM recipe (à la Noordam)

- Instrumental phase calibration
- Initial (self-)calibration and sky model
- Subtraction of outlier sources from UV data (optional peeling)
- Major calibration & imaging loop:
  - Subtraction of FoV sky model from UV data
  - Peeling of apparently bright FoV sources
  - Fitting of ionosphere model to peeling solutions
  - Application of ionosphere model during facet-based imaging & deconvolution

SPAM simplifying assumptions

- Ion. phase corruptions occur in thin layer at fixed height
- Ion. phase corruptions vary smoothly with viewing direction
- Observation integration time short enough to sample phase change rates properly
- Observation bandwidth small enough to neglect ionospheric wave dispersion
- Antennas/stations are sensitive enough to find several calibrators within target FoV
- Instrumental gains are constant in time and viewing direction throughout the observing run
- Ionospheric conditions are such that self-calibration is able to produce an initial calibration and sky model
- Processing is done on stokes I only

Instrumental phase calibration

- Dedicated observation of a flux-dominant source
- Phase calibration contains several contributions

$$\phi_{in}^{cal} = (\phi_i^{instr} + \phi_{in}^{ion}) - (\phi_r^{instr} + \phi_{rn}^{ion}) - \phi_{in}^{ambig}$$

- Iterative filtering of calibration solutions:
  - Estimation of time-constant instrumental phases

$$\tilde{\phi}_i^{instr} = \langle (\phi_{in}^{cal} - \tilde{\phi}_{in}^{ion}) \bmod 2\pi \rangle_n$$

  - Estimation of phase ambiguities

$$\tilde{\phi}_{in}^{ambig} = 2\pi \,\mathrm{round}([\tilde{\phi}_i^{instr} - \tilde{\phi}_{in}^{ion} - \phi_{in}^{cal}]/2\pi)$$

  - Fit of time-varying ionospheric phase gradient

$$\chi_n^2 = \sum_i [(\phi_{in}^{cal} - \tilde{\phi}_i^{instr} + \tilde{\phi}_{in}^{ambig}) - \underbrace{\vec{g}_n \cdot (\vec{x}_i - \vec{x}_r)}_{\tilde{\phi}_{in}^{ion}}]^2$$

Peeling

- Peeling solutions are indirect measurements of antenna-based ionospheric phase errors
- Multiple peelings (self-cal's) on FoV sources

$$\phi_{ikn}^{peel} = \phi_{ikn}^{ion} - \phi_{rkn}^{ion} - \phi_{ikn}^{ambig}$$

- External astrometric reference grid needed (NVSS, ...)
- Minimize contamination
  - Subtraction of best sky model using best calibration
  - Shortest baselines excluded from calibration
- Trade-off between #peeled sources and time-resolution
  - Variable solution interval per source + spline interpolation

Ionosphere model (1)

- Propagation “delay” causes phase error

$$\phi^{ion} \approx \frac{e^2}{4\pi\varepsilon_0 m \nu} \int n_e \, dl$$

- Interferometer measures differential phase error
- Turbulent behaviour on short spatial scales

$$D_\phi(r) = D_\phi(|\vec{r}|) = \left\langle [\phi(\vec{x}) - \phi(\vec{x}+\vec{r})]^2 \right\rangle_{\vec{x}} = (r/r_0)^\gamma$$

- Kolmogorov turbulence at ~200 km height (?)
- If dominant fluctuations occur in limited height range, a phase screen approach is justified

Ionosphere model (2)

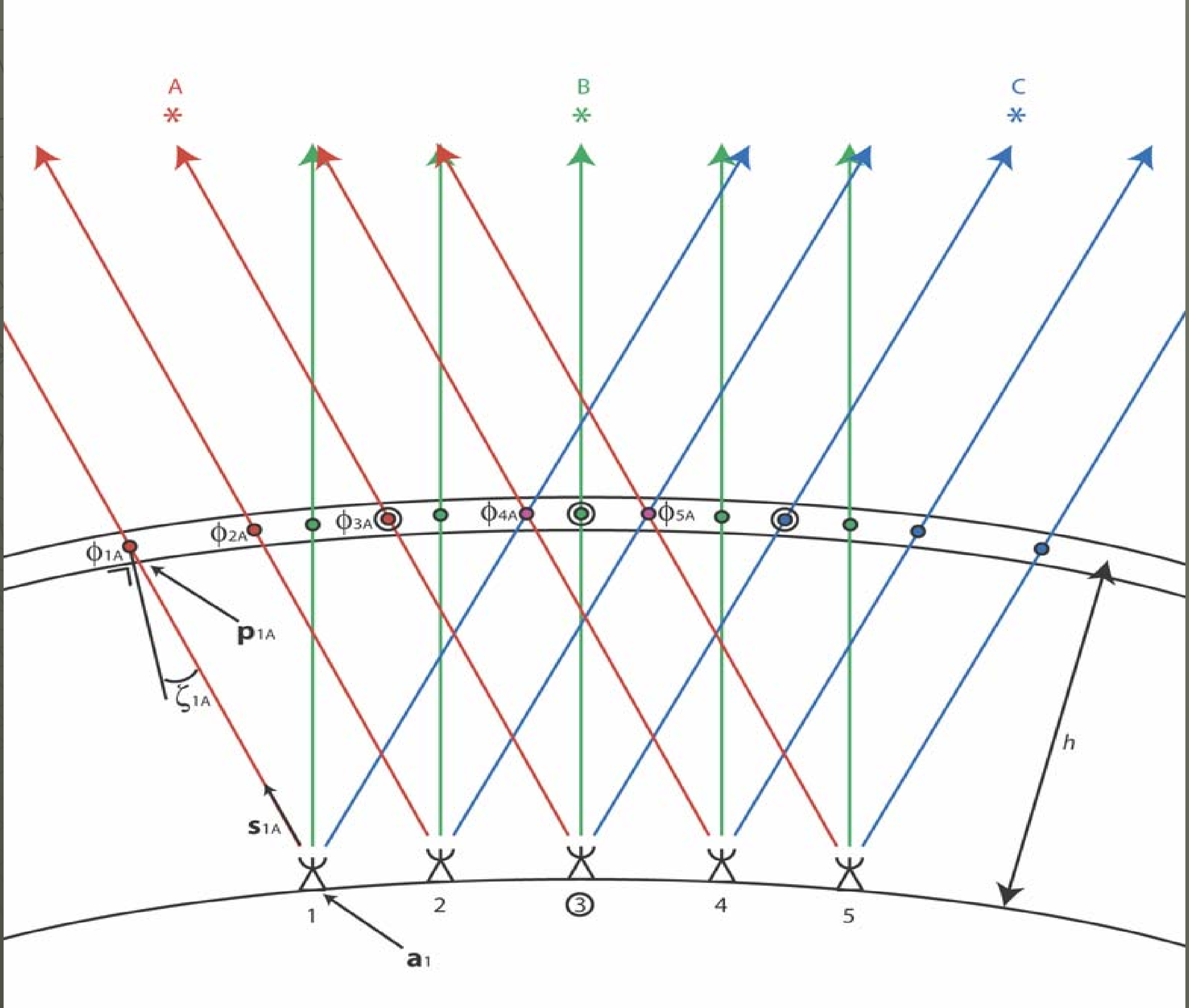

Ionosphere model (3)

- Independent phase screen per time stamp
- Airmass dependence

$$\phi^{ion}(\vec{p}_{ik}, \zeta_{ik}) = \phi^{ion}(\vec{p}_{ik}) / \cos(\zeta_{ik})$$

- Discrete Karhunen-Loeve transform (PCA)

$$\mathbf{D}_{\phi\phi} = \{(|\,\vec{p}_{ik} - \vec{p}_{i'k'}\,|)^{\gamma}\}$$

$$\mathbf{C}_{\phi\phi} = [\mathrm{diag}(\mathbf{1}_P) - \tfrac{1}{P}\mathbf{1}_P\mathbf{1}_P^{\mathrm{T}}][-\tfrac{1}{2}\mathbf{D}_{\phi\phi}][\mathrm{diag}(\mathbf{1}_P) - \tfrac{1}{P}\mathbf{1}_P\mathbf{1}_P^{\mathrm{T}}]$$

$$\mathbf{C}_{\phi\phi} = \mathbf{U}\boldsymbol{\Lambda}\mathrm{U}^{\mathrm{T}} \approx \tilde{\mathbf{U}}\tilde{\boldsymbol{\Lambda}}\tilde{\mathbf{U}}^{\mathrm{T}}$$

$$\boldsymbol{\varphi} = \{\phi^{ion}(\vec{p}_{ik})\} \approx \tilde{\mathbf{U}}\mathbf{q}$$

Ionosphere model (4)

- Find model parameters **q** by minimizing

$$\chi^2 = \sum_k \sum_i \sum_{j>i} |[\phi_{ik}^{peel} - \phi_{jk}^{peel}] - [\phi^{ion}(\vec{p}_{ik}, \zeta_{ik}) - \phi^{ion}(\vec{p}_{jk}, \zeta_{jk})] \bmod 2\pi|^2$$

- Initial guess from overall gradient fit

- Interpolation to arbitrary pierce points

$$\mathbf{D}_{\hat{\phi}\phi} = \{(|\vec{p}_{i\hat{k}} - \vec{p}_{i'k'}|)^{\gamma}\}$$

$$\mathbf{C}_{\hat{\phi}\phi} = ([-\tfrac{1}{2}\mathbf{D}_{\hat{\phi}\phi}] - [\tfrac{1}{P}\mathbf{1}_{\hat{P}}\mathbf{1}_P^{\mathrm{T}}][-\tfrac{1}{2}\mathbf{D}_{\phi\phi}])[\mathrm{diag}(\mathbf{1}) - \tfrac{1}{P}\mathbf{1}_P\mathbf{1}_P^{\mathrm{T}}]$$

$$\mathbf{C}_{\phi\phi}^{-1} = \mathbf{U}\mathbf{\Lambda}^{-1}\mathbf{U}^{\mathrm{T}} \approx \tilde{\mathbf{U}}\tilde{\mathbf{\Lambda}}^{-1}\tilde{\mathbf{U}}^{\mathrm{T}}$$

$$\hat{\boldsymbol{\varphi}} = \{\phi^{ion}(\vec{p}_{i\hat{k}})\} \approx \mathbf{C}_{\hat{\phi}\phi}\mathbf{C}_{\phi\phi}^{-1}\tilde{\mathbf{U}}\mathbf{q}$$

Ionosphere model (5)

EXAMPLE

Single time instance model fit to peeling solutions of VLA-AnB towards 7 sources

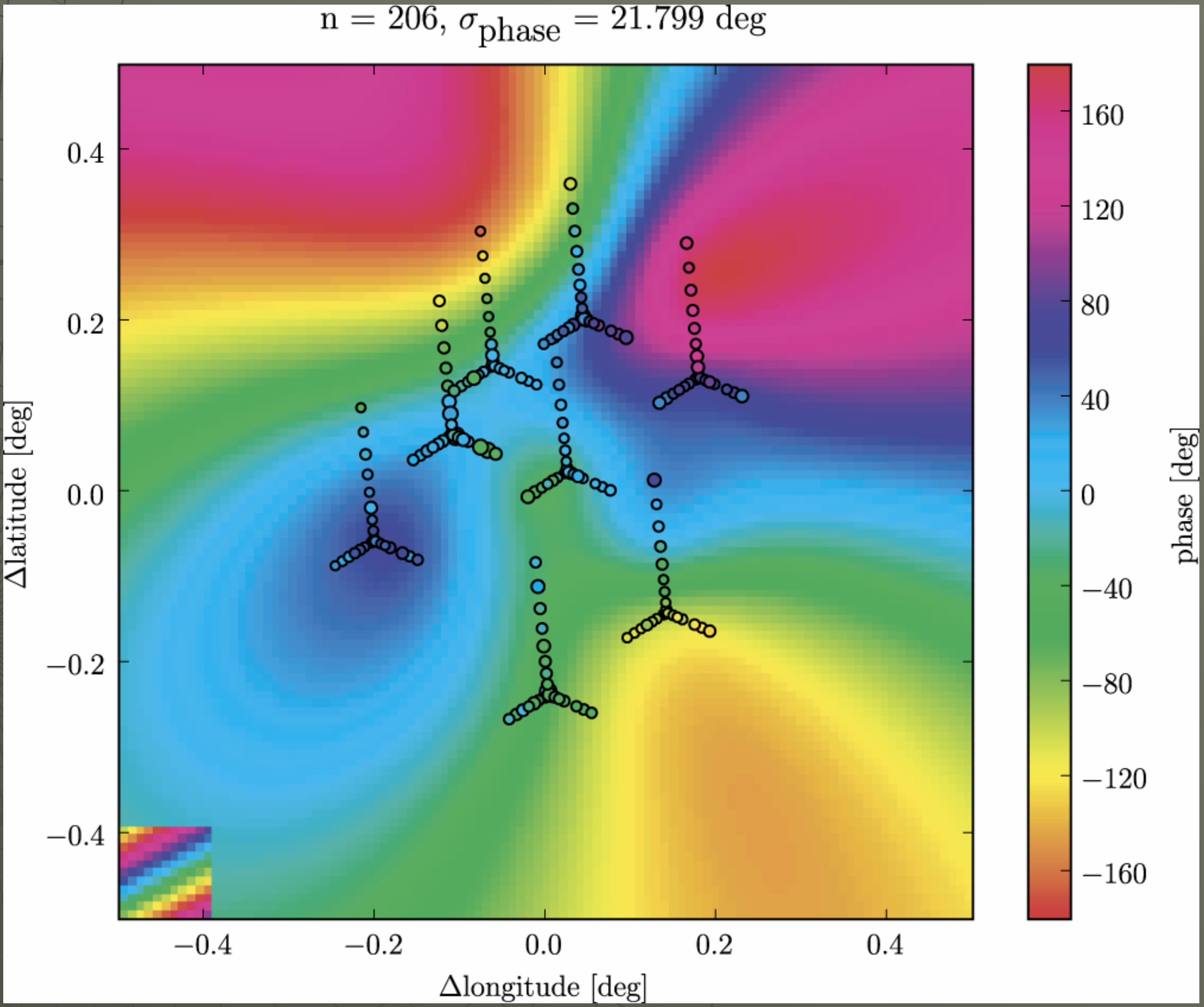

Phase comparison

EXAMPLE

Time sequences of phase solutions from different calibration schemes on 5.7 km VLA E28-W20 baseline

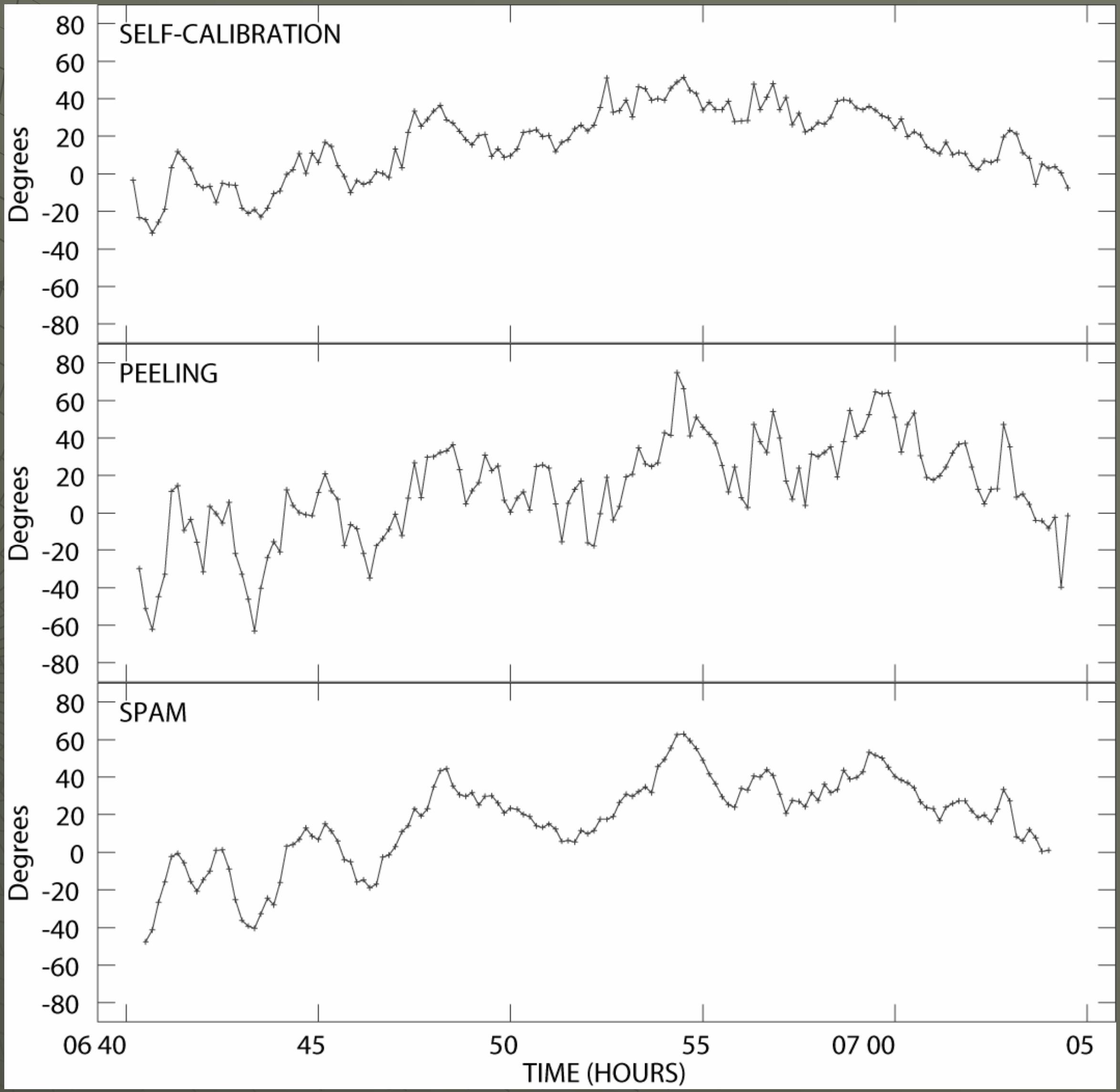

Imaging & deconvolution (1)

- No single correcting operation possible in visibility or image plane before/after imaging
- Integration into facet-based wide-field imaging
- Interpolate ion. model to each facet center
- Adjusted Cotton-Schwab major CLEAN cycle

$$I_{\hat{k}}^{res} = \mathrm{FT}[\{V_{ijn}^{res}\}] \rightarrow I_{\hat{k}}^{res} = \mathrm{FT}[\{g_{i\hat{k}n} g_{j\hat{k}n}^{+} V_{ijn}^{res}\}]$$

$$V_{ijn}^{res} - \mathrm{DFT}[\Delta I_{\hat{k}}^{mdl}]_{ij} \rightarrow V_{ijn}^{res} - (g_{i\hat{k}n} g_{j\hat{k}n}^{+})^{-1} \mathrm{DFT}[\Delta I_{\hat{k}}^{mdl}]_{ij}$$

- Optional use of raw peeling solutions for facets centered on the peeled FoV sources

Imaging & deconvolution (2)

EXAMPLE
74 MHz VLA-A
3 hrs on NGC 4565

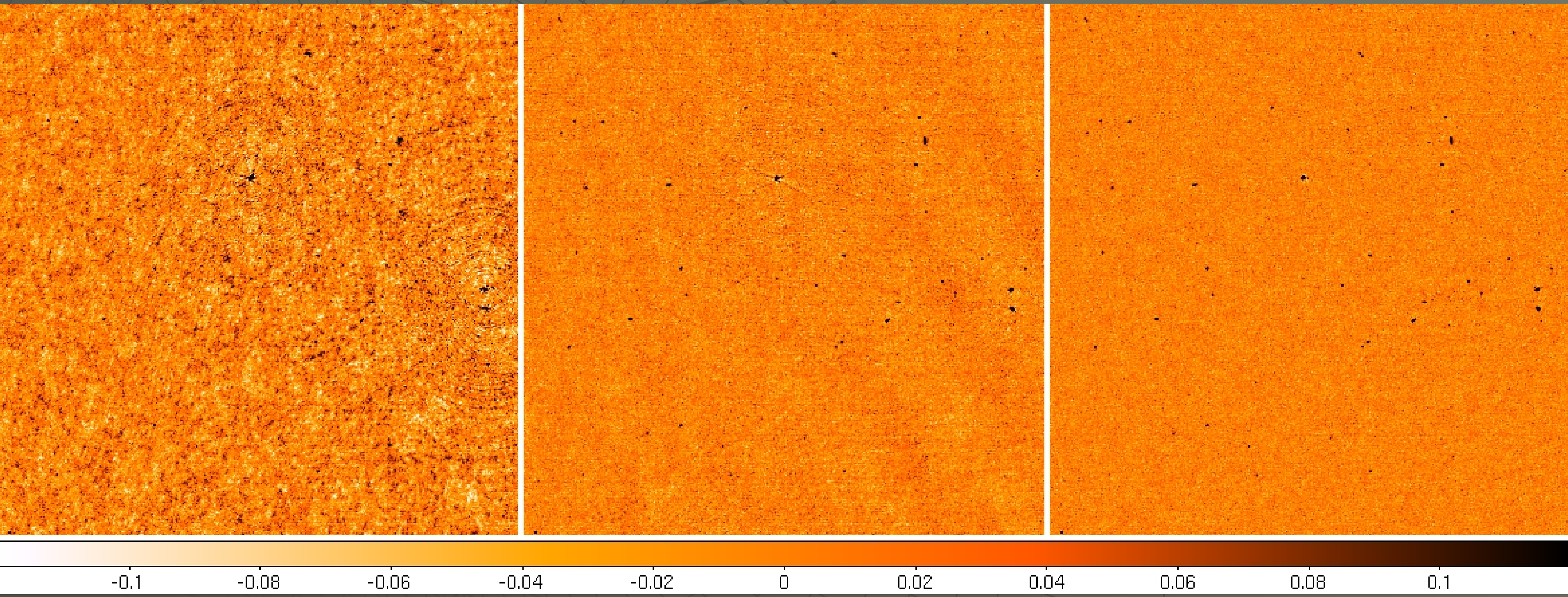

field-based calibration (2 min) self-calibration (10 sec) SPAM (10 sec)

SPAM has 5-15% higher peak fluxes down to the lowest fluxes (no Wieringa effect!)

Comparison existing calibration schemes

self-calibration	field-based calibration (Cotton et al. 2004)	SPAM (Intema et al. in prep.)
◆ antenna gain phase fixed with direction	◆ antenna gain phase varies with direction	◆ antenna gain phase varies with direction
◆ no ionospheric model	◆ measures phase gradients over array	◆ meas. higher order phase over array
	◆ phase screen at infinite height	◆ phase screen at fixed height
	◆ low order Zernike base functions	◆ higher order KL base "functions"
◆ Shortest possible time resolution	◆ 1-2 minutes time resolution	◆ Shortest possible time resolution

Areas of possible improvement

- Fine-tuning of SPAM processing parameters
- Include more complex height dependence
  - Multi-layer
- Include correlated time-behaviour
  - Kalman filtering
- Include large-scale refraction effects (most prominent at low elevations)